14th European Signal Processing Conference (EUSIPCO 2006), Florence, Italy, September 4-8, 2006, copyright by EURASIP

DIAGONAL LOADED ARRAY INTERPOLATION METHODS FOR MULTIBASELINE CROSS-TRACK SAR INTERFEROMETRY

Matteo Pardini, Fabrizio Lombardini, and Fulvio Gini

Dept of "Ingegneria dell'Informazione", University of Pisa
Via G. Caruso 14, 56122 Pisa, Italy
Tel: +39–0502217511, Fax: +39–0502217522
E-mail: pardini.matteo@bcc.tin.it, f.lombardini@iet.unipi.it, f.gini@iet.unipi.it

ABSTRACT

This work deals with the problem of interferometric radar phase (IP) estimation in the presence of multiple height layover components. The focus here is on multibaseline interferometric synthetic aperture radar (InSAR) systems with a low number of phase centres and nonuniform array geometry. Interpolated array (IA) approaches allow the application of parametric spatial spectral estimation techniques designed for uniform linear arrays (ULAs). The need for obtaining a well conditioned IA transformation matrix results in the estimation of a virtual ULA output with a number of elements lower than or equal to that of the actual non uniform linear array (NLA). Here we extend the IA approach to allow a greater number of virtual elements by means of a diagonal loading (DL) technique. The simulated performance of the proposed technique is compared with that obtained by means of another interpolation algorithm, that is optimal in a mean square error (MSE) sense, and with the Cramér-Rao lower bound (CRLB) calculated for the NLA.

1. INTRODUCTION

Interferometric synthetic aperture radar (InSAR) is a powerful technique to derive digital elevation maps (DEMs) with high spatial resolution and accuracy. Interferometry finds many applications in radar remote sensing, for topographic mapping, geology, forestry, hydrology, detection and classification of covered objects [1]. A conventional InSAR system measures the phase difference, the so-called *interferometric phase* (IP), between two SAR images collected by the antennas at the extremities of a single cross-track baseline. Unfortunately, in presence of highly sloping areas or discontinuous surfaces, this technique suffers from the layover phenomenon [1]: the received signal is the superposition of echoes backscattered from various terrain patches mapped in the same range-azimuth resolution cell (see Figure 1). Hence, the height map produced by the InSAR system is affected by strong distortion.

However, multibaseline InSAR, i.e. a technique which uses more than two SAR images, has been proposed to resolve the multiple sources along the elevation angle, see [2], [3] and references in [4]. An additional problem is the *speckle* phenomenon, caused by the possible extended nature of the backscattering sources; under some assumptions, it can be well modelled as a complex-valued multiplicative stochastic process [5]; its deleterious effects can be counteracted with the processing of more than one look. In [6] are proposed some solution to layover in the multibaseline multilook framework; several methods, including Capon, MUSIC, M-RELAX (multilook extension of RELAX) and WSF (weighted subspace fitting, see references in [4]), are tested showing satisfactory performance when a uniform linear array (ULA) structure is available.

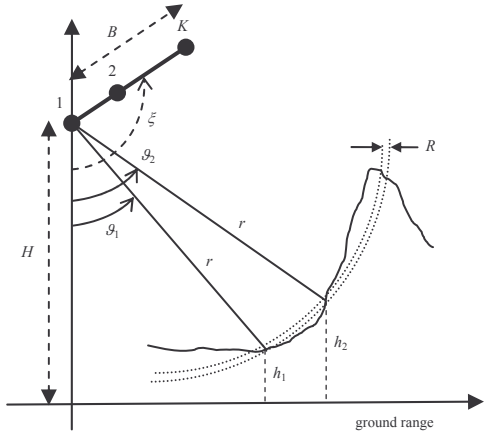

Figure 1- Geometry of the layover problem (example with two layover sources) and of interferometric system.

Unfortunately, in practical situations the ULA structure is rarely encountered, because of mechanical, structural or flight/orbital considerations, not directly related to the estimation requirements. The resulting nonuniform spatial sampling produces anomalous strong sidelobes in the elevation beam pattern and in the functional of spectral estimation methods [3], and spurious peaks and peaks misplacement can arise in presence of multiple sources [8]. As a consequence, the above mentioned approaches loose their effectiveness; also, they have a higher computational load when applied to nonuniform linear array (NLA) data.

Interpolated array (IA) approaches consist in estimating,

via linear interpolation, the output of a virtual array, typically with ULA (Vandermonde) structure, from the output of the actual array of arbitrary geometry [7]. Two are the reasons for the proposal of an IA approach in InSAR [8]. Firstly, it conveys in the interpolation mechanism a rough but correctly matched information about the overall backscattering source locations; secondly, it enables the use of the spectral estimation algorithms that for ULA structures demonstrated good performance in terms of estimation accuracy and computational efficiency.

The most commonly used IA approach is the deterministic one described by Friedlander in [7]; in [8] it has been applied to the InSAR problem for the first time. NLA structures were considered obtained by thinning a full ULA; both geometries have the same unambiguous range (UR) for IP and hence height estimation. Unfortunately, the maximum number of the virtual ULA elements which can be reconstructed is equal to the number of the actual NLA elements, because numerical ill-conditioning arises in noise whitening after array interpolation when the virtual array has more elements than those of the real one [7]. In the InSAR scenario, this fact causes a reduction of the UR, i.e. the virtual ULA does not allow to exploit all the potentialities intrinsic in NLA geometry [8]. This might be a problem in some specific multibaseline configurations and layover scenarios

The novelties of this work are the following. Firstly, we overcome the aforementioned ill-conditioning by performing a diagonal loading on the autocovariance matrix of the additive noise in the virtual ULA data, allowing it to have more elements than the actual non uniform geometry. Secondly, we apply the stochastic interpolation algorithm proposed by Choi and Munson in [9] to InSAR multibaseline array processing, ad extend it by loading, as well. Moreover, we compare the performance obtained in IP estimation by root-MUSIC applied to the virtual ULA data estimated by means of both interpolation algorithms, under different InSAR scenarios and by varying the number of elements of the virtual array. This analysis has been developed numerically using Monte Carlo simulation.

2. DATA MODEL AND PROBLEM STATEMENT

Consider a multibaseline cross-track interferometric configuration, composed of a NLA with K phase centres. The baseline length B is defined as the distance between the first and the last phase centres in the array, as shown in Figure 1. Assume that N (azimuth) looks are available; for the n-th look, $n = 1, 2, \ldots, N$, the pixel complex amplitudes collected by the array sensors from natural areas in presence of layover can be modelled as

$$\mathbf{y}(n) = \sum_{i=1}^{N_S} \sqrt{\tau_i}\,\mathbf{a}(\varphi_i) \odot \mathbf{x}_i(n) + \mathbf{v}(n) \qquad (1)$$

where $\mathbf{y}(n)$, $\mathbf{a}(\varphi_i)$, $\mathbf{x}_i(n)$ and $\mathbf{v}(n)$ are K-dimensional complex vectors, τ_i is a positive scalar, $\odot$ is the Hadamard (elementwise) product and N_S is the number of sources, i.e. the number of terrain patches with different elevation angles. Term τ_i is the radar reflectivity or texture; it is modelled as an unknown deterministic parameter. Furthermore,

$$\mathbf{a}(\varphi_i) = \begin{bmatrix} 1 & e^{jd_1\varphi_i/B} & \cdots & e^{jd_k\varphi_i/B} & \cdots & e^{j\varphi_i} \end{bmatrix}^T \qquad (2)$$

is the array steering vector of the i-th source, where d_k is the distance between the k-th sensor and the first one along the baseline and φ_i is an unknown deterministic parameter representing the IP for the i-th source in isolation, which is related to a spatial frequency [4]. In the following, for the sake of simplicity, we consider an integer NLA structure, i.e. a structure obtained by thinning a K_f element full ULA with the same aperture. The NLA phase UR, which is identical to that of the full ULA, is given by $2\pi(K_f - 1)$. The IP is related to the elevation angle ϑ_i and thus to the terrain height h_i. In fact, $\varphi_i = -4\pi B\cos(\xi - \vartheta_i)/\lambda$, where ξ is the tilt angle of the baseline and λ is the radar wavelength. Moreover, as suggested in Figure 1, $h_i = H - r\cos(\vartheta_i)$, where H is the system height and r is the range of the examined resolution cell. As a consequence, from the IPs $\{\varphi_i\}_{i=1}^{N_S}$ the heights $\{h_i\}_{i=1}^{N_S}$ of the N_S terrain patches can be reconstructed and undistorted height maps of the land surface can be produced. Vector $\mathbf{x}_i(n)$ represents the speckle distortion affecting the i-th backscattering source. It is modelled as a complex-valued correlated Gaussian process, with zero mean, unit power, and covariance matrix $\mathbf{C}_i = \mathrm{E}\{\mathbf{x}_i(n)\mathbf{x}_i^H(n)\}$. For performance analysis only, we assume that the vectors $\{\mathbf{x}_i(n)\}_{i=1}^{N_S}$ have a classical triangular shaped autocorrelation sequence [1]:

$$[\mathbf{C}_i]_{k,k+l} = \begin{cases} 1 - |d_k - d_l| b_i / B, & \text{for } |d_k - d_l| \le B/b_i \\ 0, & \text{otherwise} \end{cases} \qquad (3)$$

where $b_i = B_\perp / B_{\perp ci}$ is the normalized baseline relative to the i-th terrain patch, which depends on the radar system parameters and on the local terrain slope; $B_\perp$ denotes the baseline orthogonal to the line of sight and $B_{\perp ci}$ denotes the orthogonal critical baseline of the i-th component, i.e., the value for which the speckle of the i-th component is completely decorrelated at the extremities of the array. For $b_i = 0$ we obtain the case with constant amplitude signals along the array; b_i is a basic measure of the spatial decorrelation induced by locally flat terrain patches. It is possible to take into account also the effects of volumetric or temporal decorrelation, but they are not considered in this work. Vector $\mathbf{v}(n)$ models the additive thermal noise, a spatially white complex Gaussian process, with zero mean and power σ_v^2.

The goal here is to estimate the interferometric phases $\{\varphi_i\}_{i=1}^{Ns}$ when a rough knowledge about the overall source location is available, and $\{\tau_i\}_{i=1}^{Ns}$ and $\{\mathbf{C}_i\}_{i=1}^{Ns}$ are deterministic unknown parameters; N_S and σ_v^2 are assumed to be known.

3. DIAGONAL LOADED INTERPOLATION

Before describing how the IA approaches work and their possible extension, it is useful to comment on the choice of the virtual ULA element number K_V. It is worth remarking that in InSAR data pre-processing, the deramping procedure refers all the IPs to a selected reference [4]. As a consequence, the resulting IPs are located in a well-defined phase interval usually centred around zero; if $N_S \geq 2$, the maximum width of this interval can be expressed as $2\pi(K_f - 1)(N_S - 1)/N_S$. Unambiguous source IP estimates can be achieved if the UR of the virtual array is greater than this interval; in formulas:

$$2\pi\left(K_V - 1\right) > 2\pi\left(K_f - 1\right)\cdot\left(N_S - 1\right)/N_S \tag{4}$$

which yields a bound for K_V:

$$K_V > \frac{K_f\left(N_S - 1\right) + 1}{N_S}. \tag{5}$$

As a consequence, given K_f and N_S, it may result that $K_V = K$, as in [8] is sufficient to exploit all the NLA potentialities in terms of UR. However, greater values of K_V may be beneficial for the estimation accuracy. This issue is further investigated in Section 4.

After deramping and once a value for K_V has been selected, we can carry on with the interpolation process. In the IA approach developed by Friedlander in the early '90s [7], the virtual array output is obtained by a LS fitting with the coefficients selected so as to minimize the interpolation error over a continuous phase interval, called sector of interest (SOI), containing the true IPs of our application. More in details, define a set of s (frequency) samples uniformly spaced into the chosen sector, $[\phi_1 \;\; \phi_2 \;\; \cdots \;\; \phi_s]$; denote with $\bar{\mathbf{a}}(\phi_i)$ and $\mathbf{a}(\phi_i)$ the steering vector of the virtual and actual array, respectively [8]. Then, the output vector of the virtual array can be obtained by a $K \times K_V$ transformation matrix $\mathbf{H}_F$ by solving the least squares problem

$$\mathbf{H}_F = \arg\min_{\mathbf{H}_F} \left\| \bar{\mathbf{A}} - \mathbf{H}_F^H \mathbf{A} \right\|_{\mathrm{F}}^2 \tag{6}$$

where $\bar{\mathbf{A}} = \left[\bar{\mathbf{a}}(\phi_1) \;\; \cdots \;\; \bar{\mathbf{a}}(\phi_s)\right]$, $\mathbf{A} = \left[\mathbf{a}(\phi_1) \;\; \cdots \;\; \mathbf{a}(\phi_s)\right]$ and $\|\cdot\|_{\mathrm{F}}$ indicates the Frobenius norm. Under the assumption that $s > K$, the solution to the minimization problem stated in (6) is given by $\mathbf{H}_F = \left(\mathbf{A}\mathbf{A}^H\right)^{-1}\mathbf{A}\bar{\mathbf{A}}^H$. The $K_V \times K_V$ autocorrelation matrix of the additive noise in the virtual array data is given by $\sigma_v^2 \mathbf{H}_F^H \mathbf{H}_F$, thus this noise should be whiten if we want to estimate the IPs by means of a superresolution method such as root-MUSIC [10] or WSF [4]. Unfortunately, when $K_V > K$ the matrix $\mathbf{H}_F^H \mathbf{H}_F$ is rank deficient, thus it can not be inverted to design the whitening transformation. To overcome this problem, we propose a diagonal loading approach, carrying out the interpolation and the noise whitening as follows:

$$\bar{\mathbf{y}} = \left(\mathbf{Q}_F + \delta_F \mathbf{I}\right)^{-1} \mathbf{H}_F^H \mathbf{y} \tag{7}$$

where $\mathbf{Q}_F = \left(\mathbf{H}_F^H \mathbf{H}_F\right)^{1/2}$ and δ_F is a constant parameter, properly selected to make invertible the root of the noise autocovariance matrix, without noticeably worsen IP estimation performance (approximated whitening). Obviously, we can use $\delta_F = 0$ when $K_V \leq K$ (perfect whitening).

The other approach to array interpolation that we propose to apply in this work is a straightforward extension to the NLA InSAR case of the interpolation algorithm proposed by Munson and Choi in [9]. It was designed for the reconstruction of a band limited signal from its nonuniform samples. The only a priori knowledge on the signal that is required is its power spectral density, which in the simplest case reduces to the SOI information previously defined. To explain how the algorithm works, it is necessary to introduce two more vectors, $\mathbf{k}$ and $\bar{\mathbf{k}}$: $\mathbf{k}$ is a K-dimensional vector which describes the NLA structure, i.e. its elements are $[\mathbf{k}]_i = d_i/B$, $i = 1, 2, \ldots, K$; $\bar{\mathbf{k}}$ is analogous to $\mathbf{k}$, but it is referred to the K_V element ULA. As stated in equation (1), the vector $\mathbf{y}(n)$ can be expressed as the sum of a signal vector $\boldsymbol{\chi}(n)$, which in particular depends on the source IPs, and the thermal noise vector $\mathbf{v}(n)$. To simplify the notation, we will omit the dependence on index n in the following. In order to estimate the signal vector $\boldsymbol{\chi}_{ULA}$ of the ULA described by $\bar{\mathbf{k}}$, we want to determine a $K_V \times K$ interpolation matrix $\mathbf{H}_M$ minimizing the MSE:

$$\mathbf{H}_M = \arg\min_{\mathbf{H}_M} \mathrm{E}\left\{\left(\boldsymbol{\chi}_{ULA} - \hat{\boldsymbol{\chi}}_{ULA}\right)^2\right\} \tag{8}$$

where $\hat{\boldsymbol{\chi}}_{ULA} = \mathbf{H}_M \mathbf{y}$. This minimization involves the orthogonality principle and the solution of the well known Wiener-Hopf equation [9]. However, the exact calculation of matrix $\mathbf{H}_M$ requires knowledge of the autocorrelation sequence of $\boldsymbol{\chi}_{ULA}$, which is not available in our application. Knowledge of the SOI enables us to assume a flat signal spatial power spectral density over the frequency region corresponding to the SOI and null elsewhere; this is enough to proceed on with the interpolation. With this assumption, the solution to problem (8) is given by $\mathbf{H}_M = \mathbf{D}\left(\mathbf{B} + \eta\mathbf{I}\right)^{-1}$ [9], where $\mathbf{D}$ is a $K_V \times K$ matrix of elements $[\mathbf{D}]_{i,j} = \mathrm{sinc}[(\bar{k}_i - k_j)\beta]$ and $\mathbf{B}$ is a $K \times K$ matrix with $[\mathbf{B}]_{i,j} = \mathrm{sinc}[(k_i - k_j)\beta]$, where $\beta = \mathrm{SOI}/(2\pi)$; η is a regularization parameter which depends on σ_v^2, resulting from the solution of the Wiener-Hopf equation. Notice that the previous formulas are valid only with a null SOI central phase. The final result of the interpolation process is $\hat{\boldsymbol{\chi}}_{ULA} = \mathbf{H}_M\boldsymbol{\chi} + \mathbf{H}_M\mathbf{v}$, where $\mathbf{H}_M\mathbf{v}$ is a coloured noise vector. Similarly to what already stated about the diagonally loaded Friedlander method, this noise can not be whitened when $K_V > K$, because the $K_V \times K_V$ noise autocorrelation matrix $\sigma_v^2 \mathbf{H}_M \mathbf{H}_M^H$ is rank deficient. To solve this problem, we apply again a diagonal loading technique, which leads to the final

form of the virtual ULA data expressed below:

$$\hat{\bar{\boldsymbol{\chi}}}_{ULA} = \left(\mathbf{Q}_M + \delta_M \mathbf{I}\right)^{-1} \mathbf{H}_M \mathbf{y} \qquad (9)$$

where $\mathbf{Q}_M = \left(\mathbf{H}_M \mathbf{H}_M^H\right)^{1/2}$ and δ_M is the selected loading parameter. Again, we can use $\delta_M = 0$ when $K_V \le K$.

Once the virtual ULA output has been estimated, the root-MUSIC method for interpolated arrays [7] is employed to estimate the source IPs. More in detail, they are estimated as $(K_V - 1)$ times the angle of the N_S roots of the polynomial $f(z) = \mathbf{a}^T\left(z^{-1}\right)\mathbf{Q}^{-1}\hat{\bar{\mathbf{G}}}\hat{\bar{\mathbf{G}}}^H\mathbf{Q}^{-1}\mathbf{a}(z)$ closest to the unit circle, where the $K_V \times (K_V - N_S)$ matrix $\hat{\bar{\mathbf{G}}}$ contains the noise subspace eigenvectors of the interpolated sample correlation matrix defined as $\hat{\bar{\mathbf{R}}} = (1/N)\sum_{n=1}^{N} \boldsymbol{\gamma}(n)\boldsymbol{\gamma}^H(n)$, where $\boldsymbol{\gamma}$ is either $\bar{\mathbf{y}}$ or $\bar{\boldsymbol{\chi}}$, $\mathbf{a}(z) = [z^0 \ \cdots \ z^{K_f - 1}]^T$ and $\mathbf{Q}^{-1}$ is the noise whitening matrix.

4. NUMERICAL ANALYSIS

The performance of the two IA methods has been investigated by means of 10^4 Monte Carlo runs. Three-element NLA structures ($K = 3$, dual baseline system) are quite common in practical situations, thus we considered the array which can be obtained thinning a full ULA with $K_f = 4$; the smallest baseline is $1/3$ of the overall baseline. Using the notation introduced in the previous section, we have $\mathbf{k} = [0 \ \ 2/3 \ \ 1]$. We assumed $N_S = 2$, the maximum handled by the chosen NLA; where not otherwise stated, we also assumed a scenario with a difference between the two interferometric phases equal to $\Delta\varphi = \varphi_2 - \varphi_1 = 290°$; the other parameters were set as follows: $N = 32$, $b_1 = b_2 = 0.2$, $SNR_1 = SNR_2 = 12\text{dB}$, where $SNR_i = \tau_i / \sigma_v^2$. According to equation (5), the minimum K_V which allows to estimate the IPs unambiguously in this scenario is $K_V = K = 3$; in fact, after the deramping procedure, the maximum distance between IPs resulting from equation (4) is $\Delta\varphi_{MAX} = 540°$ and the three-element ULA has a UR of $720°$. Moreover, we assumed the deramped source IPs symmetrical with respect to the null phase, i.e. $\varphi_1 = -\varphi_2$. The Cramér-Rao lower bound (CRLB) for the NLA was also calculated (see [8] for details).

The SOI was centred around zero and its width was selected equal to $\Delta\varphi_{MAX} = 540°$ for both methods, in order to make the comparison as fair as possible, assuming for them the same a priori information about overall interferometric phase location; the samples $\{\phi_i\}_{i=1}^{s}$ were uniformly spaced in the sector with a step of 3°. We run the simulations setting $K_V = K = 3$ and $K_V = K_f = 4$; vector $\bar{\mathbf{k}}$ were equal to $[0 \ \ 1/2 \ \ 1]$ in the first case and $[0 \ \ 1/3 \ \ 2/3 \ \ 1]$ in the second. In the following, IA indicates the Friedlander method and MSE-IA indicates the Choi-Munson method, both implemented with $K_V = K = 3$; prefix DL denotes the use of diagonal loading, also implying $K_V = K_f = 4$. Moreover, we chose $\delta_F = \delta_M = 5$; extensive numerical results suggested that the estimation accuracy improves by using loading parameters relatively high, still obtaining a satisfactory whitening effect; it has also been observed that the value of reagularization parameter η does not sensibly affect the estimation performance of DL-MSE-IA.

Figures 2-4 investigate the estimation accuracy in terms of RMSE obtained by IA and MSE-IA under different InSAR scenarios, with or without diagonal loading; the curves labelled IA are a correct version of those showed in [8], where unfortunately the numerical results were slightly affected by a bug in our MATLAB code.

Fig. 2 shows the estimation accuracy as a function of $\Delta\varphi$; although DL-MSE-IA has the lowest RMSE with close sources, DL-IA is the most efficient for larger phase distances. DL-IA also gives the most accurate estimates on a wide range of source signal-to-noise ratio (Fig. 3). We observe a maximum threshold effect gain of 3 dB for intermediate values of SNR_2. In the same figure is reported also the curve obtained by applying spectral MUSIC [10] directly to the NLA data, showing that DL-IA gains more than 3 dB on spectral MUSIC. Fig. 4 shows that increasing K_V has a beneficial effect also against the source decorrelation; DL-IA is again the most efficient.

Fig. 5 reports the estimation accuracy as a function of $\Delta\varphi$ for a different array, denoted with vector $\mathbf{k} = [0 \ \ 2/7 \ \ 4/7 \ \ 1]$, with $N_S = 3$, SOI = 650º and $\delta_F = \delta_M = 5$. In this case $\Delta\varphi = \varphi_3 - \varphi_1$, $\varphi_1 = -\varphi_3$ and $\varphi_2 = 0$. Spectral MUSIC generally fails in the phase estimation with this array. When the sources are very spaced, the spurious peaks affect dramatically also the estimation performance of interpolated arrays; as a consequence, interpolating a K-element ULA could be enough even if it does not preserve the full phase UR. However, increasing K_V still provides some benefits to the accuracy of DL-IA for limited $\Delta\varphi$.

To summarize, increasing K_V generally provides more accurate estimates; DL-IA seems to be almost always the most efficient. Other simulations, not reported here for lack of space, showed that DL-IA provides nearly consistent estimates of the IPs for small normalized baselines. We remark that the SOI chosen in this work is not optimized, especially for DL-MSE-IA; in fact, narrower SOI can improve the resolution capabilities of the method. However, we considered the simplest way to convey the a priori information about the source location to the interpolation algorithm; numerical analysis proves the high efficiency of DL-IA with this choice.

5. CONCLUSIONS

We tackled the problem of interferometric phase estimation of InSAR signals in presence of layover for systems with a low number of phase centres and NLA geometry. We extended the deterministic interpolated array approach for

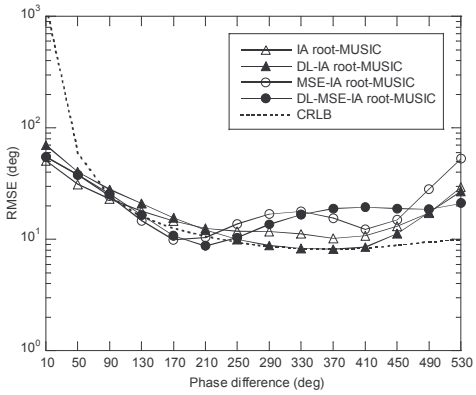

Figure 2 – **k** = [0 2/3 1], estimation of φ_2. RMSE of interpolated array methods as a function of $\Delta\varphi$.

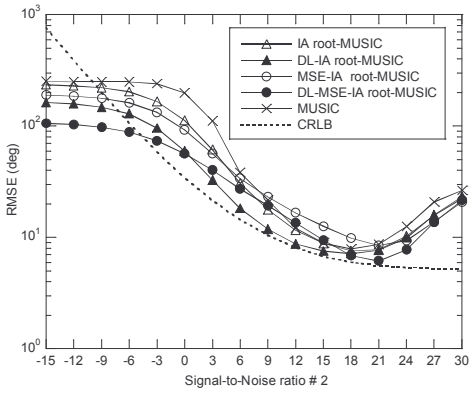

Figure 3 – **k** = [0 2/3 1], estimation of φ_2. RMSE of interpolated array methods as a function of SNR_2.

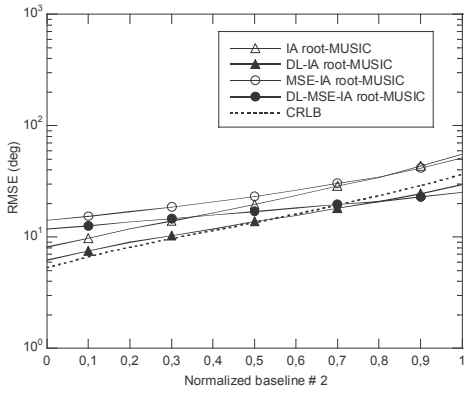

Figure 4 – **k** = [0 2 3], estimation of φ_2. RMSE of interpolated array methods as a function of b_2.

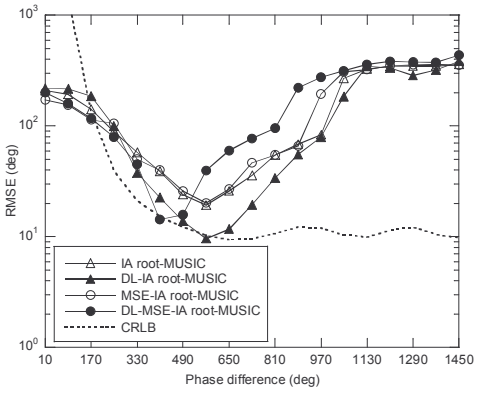

Figure 5 – **k** = [0 2/7 4/7 1], estimation of φ_2. RMSE of interpolated array methods as a function of $\Delta\varphi$.

the reconstruction of a virtual ULA with a number of elements greater than that of the actual NLA, by means of a diagonal loading approach (DL-IA). We compared its IP estimation performance with that obtained by another interpolation method, the MSE-IA, based on the minimization of the interpolation MSE; the comparison was carried out under different InSAR scenarios and for different values of K_V, the number of virtual ULA elements. In both cases, IP estimation has been performed by means of root-MUSIC. The numerical analysis showed that selecting K_V greater than the maximum classical value brings a beneficial effect on estimation accuracy. Also, the unambiguous height range of the NLA is preserved. However, when the layover components are very spaced – a case which is not so common – accuracy is not good. DL-IA is the most accurate IP estimator in most of the simulated scenarios we considered, and it is always pretty close to the CRLB calculated for the NLA.

REFERENCES

[1] E. Rodriguez and J.M. Martin, "Theory and Design of Interferometric Synthetic Aperture Radars", *IEE Proceedings-F*, vol. 139, pp. 147-149, April 1992.

[2] P. Pasquali, C. Prati, F. Rocca and M. Seymour, "A 3D SAR Experiment with EMSL Data", *IEEE Geoscience and Remote Sensing Symposium 1995* (IGARSS'95), July 1995, Florence, Italy.

[3] F. Lombardini and A. Reigber, "Adaptive Spectral Estimation for Multibaseline SAR Tomography with Airborne L-band Data", *IEEE Geoscience and Remote Sensing Symposium 2003* (IGARSS'03), July 2003, Tolouse, France.

[4] F. Gini and F. Lombardini, "Multibaseline Cross-Track SAR Interferometry: A Signal Processing Perspective," *IEEE Trans. on Aerospace and Electronic Systems*, *Tutorials II,* vol. 20, No. 8, pp. 71-93, August 2005.

[5] F.M. Henderson and A.J. Lewis, *Manual of Remote Sensing, Vol. 2, Principle and Applications of Imaging Radar*, 3rd ed., Englewood Cliffs, NJ: Prentice Hall, 1998.

[6] F. Gini, F. Lombardini and M. Montanari, "Layover Solution in Mutibaseline SAR Interferometry", *IEEE Trans. on Aerospace and Electronic Systems*, vol. 38, pp. 1344-1356, October 2002.

[7] B. Friedlander, "The root-MUSIC Algorithm for Direction Finding with Interpolated Arrays", *Signal Processing*, vol. 30, pp. 15-29, January 1993.

[8] F. Bordoni, A. Jakobsson, F. Lombardini, and F. Gini, "Multibaseline Cross-Track SAR Interferometry using Interpolated Arrays", *IEEE Trans. on Aerospace and Electronic Systems*, vol. 41, No. 4, pp. 1472-1481, October 2005.

[9] H. Choi and D.C. Munson Jr., "Stocastic Formulation of Bandlimited Signal Interpolation", *IEEE Trans. on Circuits and Systems – II: Analog and Digital Signal Processing*, vol. 47, pp. 82-85, January 2000.

[10] P. Stoica and R. Moses, *Introduction to Spectral Analysis*, Englewood Cliffs, NJ: Prentice Hall, 1997